Pairing state at an interface of Sr_2RuO_4: parity-mixing, restored time-reversal symmetry, and topological superconductivity

Y. Tada, N. Kawakami, and S. Fujimoto

Department of Physics, Kyoto University, Kyoto 606-8502, Japan

Abstract. We investigate pairing states realized at the (001) interface of a spin-triplet superconductor Sr_2RuO_4 on the basis of microscopic calculations. Because of a Rashba-type spin-orbit interaction induced at the interface, strong parity-mixing of Cooper pairs between a spin-singlet state and a spin-triplet state occurs in this system. There are also strong inter-band pair correlations between the spin-orbit split bands, in spite of the considerably large spin-orbit splitting. This is due to frustration between the spin-orbit interaction and pairing interactions. In this pairing state, time-reversal symmetry is restored, in contrast to the bulk Sr_2RuO_4 which is believed to be a chiral $p + ip$ superconductor with broken time-reversal symmetry. It is demonstrated that, because of these features, the pairing state at the interface is a promising candidate for the recently proposed time-reversal invariant topological superconductor.

1. Introduction

In unconventional superconductors, the BCS order parameter possesses internal degrees of freedom, which give rise to various rich physics, as explored for Helium 3 [1], Sr_2RuO_4 [2, 3], and heavy fermion superconductors [4, 5]. For Sr_2RuO_4, a possible realization of a chiral $p + ip$ pairing state is suggested by several experimental and theoretical studies [3, 6, 7]. In this p-wave pairing state, time-reversal symmetry is broken by orbital degrees of freedom. Because of this feature, the chiral $p + ip$ superconductor bears some similarities to the quantum-Hall-effect (QHE) state [8]. For instance, in a chiral $p + ip$ superconductor with open boundaries, a gapless edge mode propagating in only one direction appear at the boundary edges, which is in analogy with a chiral edge state in the QHE state. This similarity ultimately stems from the realization of a topological state in both of these quantum condensed phases. A topological state is a novel class of quantum ground state which is characterized not by conventional long-range order, but by a topologically nontrivial structure of the Hilbert space. In a topological state, there is a bulk excitation energy gap which ensures the stability of this state, and, as mentioned above, there are also gapless edge states which play an important role for transport phenomena. In the case with broken time-reversal symmetry such as the QHE state and the chiral $p + ip$ superconductors, the topological structure is associated with the existence of a nonzero topological number, i.e. the Chern number [9]. Recently, another class of a topological state was theoretically proposed for band insulators [10, 11, 12] and experimentally observed [13]. This topological state, which is called the Z_2 topological insulator, possesses time-reversal symmetry, in contrast to the above-mentioned topological state without time-reversal symmetry, and is characterized by the existence of two counter-propagating gapless edge modes, which are associated with the Kramers doublet. These gapless edge modes give rise to the quantum spin Hall effect, which has been attracting recently much interest in connection with possible applications to spintronics. As there is similarity between the chiral $p + ip$ superconductors and the QHE state, there is parallelism between the Z_2 topological insulator and noncentrosymmetric p-wave superconductors [14, 15, 16, 17, 18, 19]. In these few years, many classes of noncentrosymmetric superconductors (NCSC), the crystal structures of which lack inversion symmetry, have been discovered [20, 21, 22, 23, 24, 25]. Some experimental and theoretical studies suggest that p-wave pairing states may be realized in certain systems of NCSC such as $CePt_3Si$ and Li_2Pt_3B [26, 27, 28]. However, unfortunately, these NCSC are not suitable for the realization of the Z_2 topological phase, because their superconducting gaps possess nodes [29, 27], from which gapless quasiparticles in the bulk appear, and destabilize the topological state.

In this paper, we investigate a possible realization of the Z_2 topological superconductivity at an interface of Sr_2RuO_4. We consider the (001) interface, at which the Rashba-type spin-orbit (SO) interaction breaking inversion symmetry may be induced [30]. We can also consider a setup in which a thin film of Sr_2RuO_4 is

fabricated on a substrate with a bias potential applied perpendicular to the (001) interface, which controls the strength of the Rashba SO interaction. Apart from the exploration of the Z_2 topological superconductivity, such a system is interesting in that it is suitable for the systematic investigation on the effect of party-mixing of pairing states raised by broken inversion symmetry [31, 32]. For the realization of substantial parity-mixing of Cooper pairs, the existence of attractive interactions in both spin-singlet and spin-triplet channels is crucially important. Sr_2RuO_4 is a good candidate for the realization of such a situation, because, according to microscopic analysis on the mechanism of superconductivity for this system, both the p-wave channel and the d-wave channel enjoy substantially strong attractive interactions [33, 34]. It is expected that the addition of the asymmetric SO interaction to this system raises the strong admixture of spin-singlet pairs and spin-triplet pairs. In general, the structure of the parity-mixed Cooper pairs is determined by competition between the asymmetric SO interaction and pairing interactions in each channel [31, 35, 36, 37]. When the asymmetric SO interaction is dominant, the structure of the $\boldsymbol{d}$-vector for the spin-triplet component is mainly constrained by the SO interaction to suppress pairings between two SO split bands, which are unfavorable when the SO split is much larger than the superconducting gap. However, in the case that the pairing interaction that is not compatible with the symmetry of the asymmetric SO interaction is dominant, the direction of the $\boldsymbol{d}$-vector does not minimize the energy cost due to the asymmetric SO interaction, yielding inter-band pairings between the SO split bands. For the case of Sr_2RuO_4, the dominant pairing interaction exists in the p-wave channel, and the $\boldsymbol{d}$-vector is perpendicular to the xy-plane because of the bulk SO interaction of the d-electron orbitals [3, 33, 38, 39]. In this paper, we consider the case that the asymmetric SO interaction at the interface is stronger than the bulk SO interaction, and examine how the chiral $p+ip$ state in the bulk is affected by the asymmetric SO interaction, and what pairing symmetry is most stabilized at the interface. This is another purpose of the current paper.

Our main results are as follows. As the asymmetric SO interaction becomes strong, the $\boldsymbol{d}$-vector of the p-wave pairing is oriented to directions parallel to the xy-plane. However, there exists strong frustration between the asymmetric SO interaction and the p-wave pairing interaction because of an additional anisotropic structure of the pairing interaction. Thus, the direction of the $\boldsymbol{d}$-vector does not fully optimize the asymmetric SO interaction, inducing substantial amount of Cooper pairs between the two SO split bands, in spite of the SO splitting much larger than the superconducting gap. As a result, the stable pairing state possesses $p+d$ wave symmetry, rather than $s+p$ wave symmetry or $d+f$ wave symmetry which is expected to be stabilized for the Rashba superconductors when the inter-band pairs are suppressed [31, 35, 36]. The notable feature of the $p+d$ wave state is that the single-particle energy has a full gap, and there are no nodal excitations for small strength of the asymmetric SO interaction. Furthermore, since the $\boldsymbol{d}$-vector is parallel to the xy-plane, *time-reversal symmetry is restored*, which makes sharp contrast with the chiral superconductivity realized in the bulk of Sr_2RuO_4. These two features are quite important for the realization of the Z_2

topological superconductivity mentioned above. We can show that the pairing state realized at the interface is topologically equivalent to the combined state of a $p + ip$ state and a $p - ip$ state, which is time-reversal invariant, and supports the existence of counter-propagating gapless edge modes, which carry spin currents.

The organization of this paper is as follows. In the sections 2 and 3, the pairing state at the interface of Sr_2RuO_4 is microscopically investigated on the basis of the scenario that the pairing interaction is caused by electron correlation effects. We analyse the structure of the parity-mixed pairing gap. In the section 4, exploiting the results obtained in the section 3, we present a possible scenario for the realization of the Z_2 topological superconductivity in this system. Discussion and summary are given in the last section.

2. Model and formulation

In this section, we introduce a low-energy effective model for superconductivity realized at an interface of Sr_2RuO_4, and present a theoretical framework used for the study on pairing states.

2.1. Low-energy effective model

In Sr_2RuO_4, there exist three quasi 2-dimensional orbitals Ru4d$_{xy,xz,yz}$ in RuO_2 plane for electrons which play the most significant roles for low-energy properties. There are several theoretical proposals for the microscopic origin of pairing interaction in Sr_2RuO_4 [2, 3]. One of promising scenarios is that an effective pairing interaction in the p-wave channel is produced by higher order processes of electron-electron interaction through the Kohn-Luttinger-type mechanism [33]. In this scenario, which is first proposed by Nomura and Yamada, among the three bands, α, β and γ-band formed by the t_{2g} orbitals, the γ-band originating from the d$_{xy}$ orbital is considered to be most important for the realization of the superconductivity. In this paper, we employ this scenario, because this appraoch enables us to calculate the transition temperature which is quantitatively in good agreement with experimental observations. Therefore, to discuss the appearance of superconductivity, it is sufficient to focus only on the γ-band. Although there exists the SO interaction between the t_{2g} orbitals (we call this SO interaction the bulk SO interaction) which tends to direct the $\boldsymbol{d}$-vector parallel to the z-axis, its effective energy scale for the pinning of the $\boldsymbol{d}$-vector is small and negligible for a discussion on the transition temperature T_c. However, for electrons near the surface or an interface parallel to RuO_2 plane, there exists another kind of spin-orbit interaction called the asymmetric SO interaction which breaks both reflection symmetry in the momentum space $\boldsymbol{k} \to -\boldsymbol{k}$ and spin rotation symmetry. This SO interaction originates from the spin-flip hopping processes between the Ru t_{2g} orbitals, of which the wave functions are modulated by a potential gradient in the vicinity of an interface. For the superconductivity, it tends to make the direction of the $\boldsymbol{d}$-vector perpendicular to the

z-axis as shown in section3. In the following analysis, we assume that the asymmetric SO interaction is sufficiently stronger than the bulk SO interaction, and neglect effects of the bulk SO interaction.

We, then, simply describe the electrons of the γ-band near an interface by the single band Hubbard model,

$$H = \sum_k c_k^\dagger [\varepsilon_k + \alpha \boldsymbol{\mathcal{L}}_0(\boldsymbol{k}) \cdot \boldsymbol{\sigma}] c_k + U \sum_i n_{i\uparrow} n_{i\downarrow}, \tag{1}$$

where $c_k = (c_{k\uparrow}, c_{k\downarrow})^t$ is the annihilation operator and $n_{i\sigma} = c_{i\sigma}^\dagger c_{i\sigma}$. The asymmetric type SO interaction induced near the (001)-interface is incorporated into the first term of the Hamiltonian. The strength of the asymmetric SO interaction is denoted by α. We assume that the Rashba form of the asymmetric SO interaction [30]. For Sr_2RuO_4, the dispersion relation ε_k and the Rashba type SO interaction are approximated by

$$\varepsilon_k = -2t_1(\cos k_x + \cos k_y) + 4t_2 \cos k_x \cos k_y - \mu, \tag{2}$$

$$\boldsymbol{\mathcal{L}}_0(\boldsymbol{k}) = (\sin k_y, -\sin k_x, 0). \tag{3}$$

The parameters are fixed as $(t_1, t_2) = (1.0, -0.375)$ taking t_1 as the energy unit, and the filling is $n = 1.32$. The hopping integral and the electron density are chosen so that the Fermi surface of our model is consistent with the experiments. In the real system, the form of $\boldsymbol{\mathcal{L}}_0(\boldsymbol{k})$ may be more complicated. However, as will be shown in the section 3, this simplified model captures important physics raised by broken inversion symmetry.

2.2. Perturbation theory for the Kohn-Luttinger mechanism of superconductivity

There are some theoretical proposals for the mechanism of p-wave superconductivity realized in Sr_2RuO_4. One promising scenario is that the pairing interaction in this system is caused by the Kohn-Luttinger mechanism; higher order interaction processes due to the Coulomb interactions U give rise to effective pairing interactions in interaction channels with nonzero angular momentum [40]. Actually, Nomura and Yamada demonstrated that interaction processes up to the third order in U yield a strong pairing interaction in the p-wave channel for the microscopic model of Sr_2RuO_4. This scenario successfully explains the origin of the p-wave superconductivity realized in this system. We, here, apply this perturbation theory for the pairing interaction to the model (1).

For this purpose, we introduce noninteracting Green's function,

$$G_{\alpha\beta}^0(k) = \sum_{\tau=\pm1} l_{\tau\alpha\beta}^0(k) G_\tau^0(k), \tag{4}$$

$$l_{\tau\alpha\beta}^0(k) = \frac{1}{2}\left(1 + \tau \hat{\boldsymbol{\mathcal{L}}}_0(\boldsymbol{k}) \cdot \boldsymbol{\sigma}\right)_{\alpha\beta}, \tag{5}$$

$$G_\tau^0(k) = \frac{1}{i\omega_n - \varepsilon_{k\tau}}, \tag{6}$$

where $\varepsilon_{k\tau} = \varepsilon_k + \tau\alpha|\boldsymbol{\mathcal{L}}_0(\boldsymbol{k})|$, $\hat{\boldsymbol{\mathcal{L}}}_0(\boldsymbol{k}) = \boldsymbol{\mathcal{L}}_0(\boldsymbol{k})/|\boldsymbol{\mathcal{L}}_0(\boldsymbol{k})|$ and $|\boldsymbol{\mathcal{L}}_0(\boldsymbol{k})| = \sqrt{\sum_{i=1}^3 [\mathcal{L}_{0i}(\boldsymbol{k})]^2}$. ω_n is the fermionic Matsubara frequency. As seen in the form of $G_{\alpha\beta}^0$, the Fermi surface splits into two bands whose dispersions are ε_+ and ε_- with the splitting $\sim \alpha/v_F$ (v_F is

the averaged Fermi velocity of the two bands). Note that $\boldsymbol{\mathcal{L}}_0 = 0$ at the van Hove points $(0, \pm\pi), (\pm\pi, 0)$ and the Fermi surface is changed little around them since the Rashba SO interaction is small there.

The effective pairing interaction is expanded up to the third order with respect to U. It is expressed as,

$$
\begin{aligned}
V_{\sigma_1\sigma_2\sigma_3\sigma_4}(k,k') &= \frac{1}{2}[V^{\mathrm{RPA}}_{\sigma_1\sigma_2\sigma_3\sigma_4}(k,k') + V^{\mathrm{Ver}}_{\sigma_1\sigma_2\sigma_3\sigma_4}(k,k')],\\
V^{\mathrm{RPA}}_{\sigma\bar{\sigma}\sigma\bar{\sigma}}(k,k') &= U + U^2\chi^0(k+k') + U^3[\left(\chi^0(k-k')\right)^2 + \left(\chi^0(k+k')\right)^2],\\
V^{\mathrm{Ver}}_{\sigma\bar{\sigma}\sigma\bar{\sigma}}(k,k') &= 2U^3\mathrm{Re}\sum_q G^0_{\sigma\sigma}(-k+q)[\chi^0(q)G^0_{\sigma\sigma}(-k'+q) - \phi^0(q)G^0_{\sigma\sigma}(k'+q)],\\
V^{\mathrm{RPA}}_{\sigma\sigma\sigma\sigma}(k,k') &= -U^2[\chi^0(k-k') - \chi^0(k+k')],\\
V^{\mathrm{Ver}}_{\sigma\sigma\sigma\sigma}(k,k') &= 2U^3\mathrm{Re}\sum_q G^0_{\sigma\sigma}(k+q)[\chi^0(q) + \phi^0(q)][G^0_{\sigma\sigma}(k'+q) - G^0_{\sigma\sigma}(-k'+q)],\\
V_{\sigma\bar{\sigma}\bar{\sigma}\sigma}(k,k') &= -V_{\sigma\bar{\sigma}\sigma\bar{\sigma}}(k,-k'),\\
\text{others} &= 0,
\end{aligned}
$$

where

$$\chi^0(q) = -\frac{T}{N}\sum_k G^0_{\sigma\sigma}(q+k)G^0_{\sigma\sigma}(k), \tag{7}$$

$$\phi^0(q) = -\frac{T}{N}\sum_k G^0_{\sigma\sigma}(q-k)G^0_{\sigma\sigma}(k), \tag{8}$$

and $k = (\omega_n, \boldsymbol{k})$, and T and N are, respectively, temperature and the number of Ru sites. χ^0 and ϕ^0 do not depend on spins because $G^0_{\uparrow\uparrow}(k) = G^0_{\downarrow\downarrow}(k)$ is satisfied. We, here, neglect many terms in V which arise from non-zero off-diagonal elements of Green's function $G_{\sigma\bar{\sigma}}(k)$, because $G_{\sigma\bar{\sigma}}(k)$ is smaller than $G_{\sigma\sigma}$ by the factor of α/ε_F where ε_F is the Fermi energy. Besides, the terms in V with spin-flip processes represent the perturbative effects of the Rashba SO interaction and, in itself, do not have crucial importance as long as $\alpha \ll \varepsilon_F$. Each $V_{\sigma_1\sigma_2\sigma_3\sigma_4}$ consists of the RPA-like terms V^{RPA} and the vertex-correction terms V^{Ver}. The former is included within random phase approximation(RPA), and the latter is not. For spin-singlet pairing, the RPA-like terms give dominant attractive interaction and play significant roles for its stability, while the vertex-correction terms do for triplet pairing.

The transition temperatures for the superconductivity are calculated by solving the linearized Eliashberg equation

$$\lambda\Delta_{\alpha\alpha'}(k) = -\frac{T}{N}\sum_k V_{\alpha\alpha'\beta\beta'}(k,k')G^0_{\beta\gamma}(k')G^0_{\beta'\gamma'}(-k')\Delta_{\gamma\gamma'}(k') \tag{9}$$

where Δ is the anomalous self-energy and λ is the eigenvalue. We identify the temperature for which $\lambda(T) = 1$ as the transition temperature. The normal self-energy is neglected because it is not important in the present study. In this equation, spin-flip processes are included only in the factor $G(k)G(-k)$ and are not in V within our approximation. This is because the factor $G(k)G(-k)$ behaves like a window function which allows electrons only near the Fermi surface to participate in the superconductivity

and therefore has non-perturbative effects of the Rashba SO interaction, while the spin-flip scattering processes in V are perturbative. We note that some of the elements of $G^0_{\beta\gamma}(k)G^0_{\beta'\gamma'}(-k)$ are strongly anisotropic in the $\boldsymbol{k}$-space, which restrict the possible symmetries of the gap functions. Furthermore, these elements with $\beta \neq \beta'$ or $\gamma \neq \gamma'$ give rise to parity-mixing between spin-singlet and spin-triplet pairs, which is one of the most remarkable features of NCSC.

The anomalous self-energy is generally written as,

$$\Delta(k) = [D_0(k) + \boldsymbol{D}(k) \cdot \boldsymbol{\sigma}]i\sigma_2, \tag{10}$$

where $D_0(k)$ and $\boldsymbol{D}(k)$ are the singlet and triplet parts, respectively, and the $\boldsymbol{k}$-dependence of $D_\mu(i\omega_n, \boldsymbol{k})$ represents the symmetry of the superconductivity. The structure of the $\boldsymbol{d}$-vector $\boldsymbol{D}$ is determined by the two factors. One is the pairing interaction V and, in the case of Rashba superconductors, there exists the other factor $\boldsymbol{\mathcal{L}}_0$. The microscopic origins of these two factors are generally different, and the $\boldsymbol{d}$-vector which V favors does not necessarily coincide with the one which $\boldsymbol{\mathcal{L}}_0$ favors. For sufficiently large α with $D_\mu \ll \alpha \ll \varepsilon_F$, the most stable direction of the $\boldsymbol{d}$-vector is $\boldsymbol{D} \parallel \boldsymbol{\mathcal{L}}_0$ because, if this condition is satisfied, $\Delta(k)$ in the matrix form can be diagonalized with respect to the $\tau = \pm$ bands. Conversely, when $\boldsymbol{D}$ is not parallel to $\boldsymbol{\mathcal{L}}_0$, inter-band pairs between the SO split bands are induced, which generally lead to pair-breaking effects. In contrast, for enough small α, the structure of $\boldsymbol{D}$ is determined by the pairing interaction. Generally, these two factors which can determine the structure of the $\boldsymbol{d}$-vector compete with each other. In the next section, we discuss the effects of the Rashba SO interaction on the transition temperature and the structure of D_μ.

To solve the Eliashberg equation (9) numerically, we divide the Brillouin zone into 64×64 meshes and take 1024 Matsubara frequencies.

3. Results for the pairing state

In this section, we present the results for stable pairing states and their transition temperatures calculated by using the formulation given in the section 2.

3.1. Structure of pairing interaction

We first show the momentum profile of $\chi^0(q)$ in figure 1 for $\alpha = 0$ and $\alpha = 0.1$ at $T = 0.01$, which plays an important role for the pairing mechanism. The difference in χ^0 for $\alpha = 0$ and $\alpha = 0.1$ are so small that the $\boldsymbol{k}$-dependence of V is also changed little by the Rashba SO interaction. Indeed, we have confirmed that the $\boldsymbol{k}$-dependence of V is almost unchanged at least up to $\alpha \sim 0.1$. This means that, in view of the pairing interaction, the most stable symmetry of the superconductivity for $\alpha = 0$ is stable also for $\alpha \neq 0$. As shown in figure 2, however, the amplitude of the pairing interaction for the triplet part $V_t = \frac{1}{2}[V^{\mathrm{RPA}}_{\sigma\sigma\sigma\sigma} + V^{\mathrm{Ver}}_{\sigma\sigma\sigma\sigma}]$ is decreased for large α, because the main part of V_t is V^{Ver} which is sensitive to the electronic structure. On the other hand, the interaction for the singlet part $V_s = [V^{\mathrm{RPA}}_{\sigma\bar{\sigma}\sigma\bar{\sigma}} + V^{\mathrm{Ver}}_{\sigma\bar{\sigma}\sigma\bar{\sigma}}]$ is not so changed, since V_s is

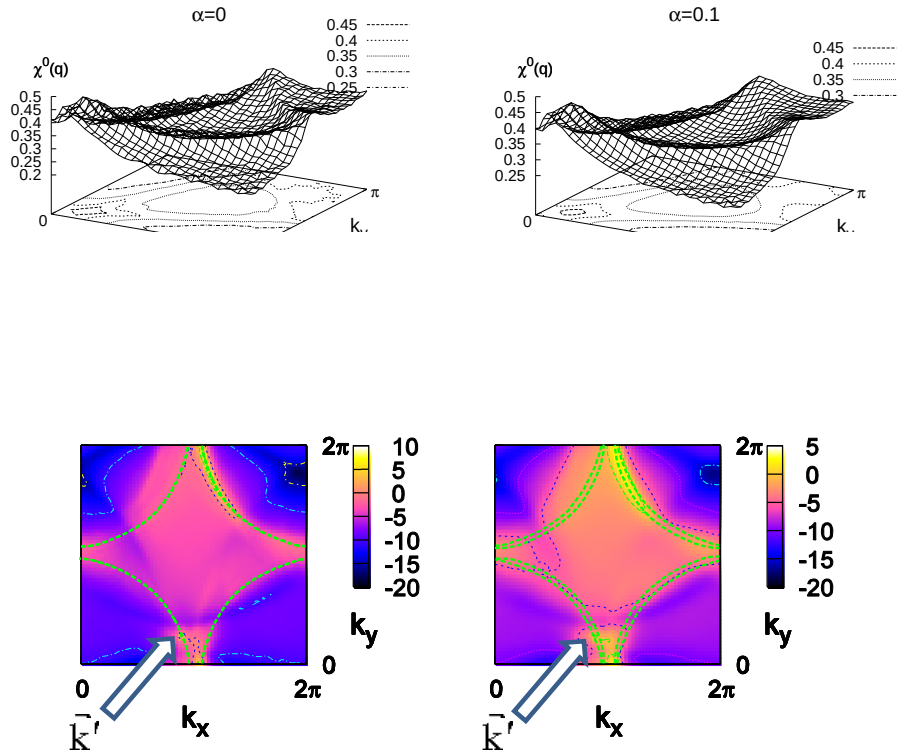

Figure 2. Plot of the pairing interaction $V_t(k, k')$ on the $\boldsymbol{k} = (k_x, k_y)$ plane with fixed $\boldsymbol{k}'$ at $T = 0.01, U = 5.5$, for $\alpha = 0$ (left panel) and $\alpha = 0.1$ (right panel). Here the Matsubara frequencies which appear in V_t is fixed as $\nu_n = \nu'_n = i\pi T$. $\boldsymbol{k}'$ is fixed as illustrated in the figure.

mainly determined by V^{RPA} which is directly related to the α-insensitive function χ^0. Therefore, it is expected that the triplet superconductivity would be suppressed while the singlet superconductivity unaffected through the change in V by the Rashba SO interaction. However, as mentioned before, the Rahsba SO interaction has the other important effects on T_c which are non-perturbative in the sense that $G(k)G(-k)$ strongly restricts the possible symmetries of the gap functions, and gives rise to parity-mixing of Cooper pairs.

3.2. Pairing state and transition temperature in the case without parity-mixing

As mentioned above, there are two important effects of the Rashba SO interaction on pairing states: one is to constrain the direction of the $\boldsymbol{d}$-vector of spin-triplet pairings, and the other is parity-mixing. We, first, examine the former effect, neglecting the effect of parity-mixing for a while. Actually, the parity-mixing is not negligible in the present study, and will be discussed in the next subsection.

Neglecting the terms which mix the singlet and the triplet gap functions in the Eliashberg equation (9), we calculated the transition temperatures T_c for the spin-singlet channels and for the spin-triplet channels separately. We also computed the

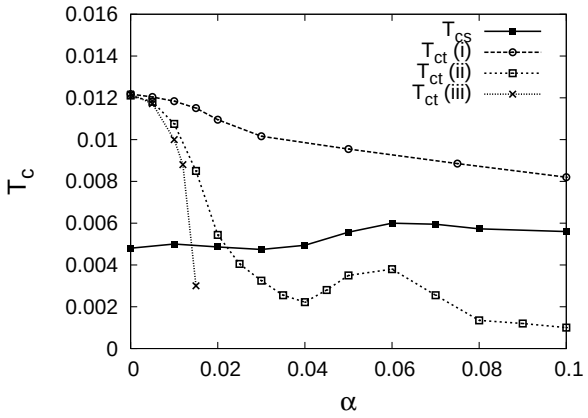

Figure 3. α versus T_{cs} and T_{ct} at $U = 5.5$. The gap functions roughly expressed as $D_0 \sim (\cos k_x - \cos k_y)$ for T_{cs}, $\boldsymbol{D} \sim (-\cos k_x \sin k_y \hat{x} + \cos k_y \sin k_x \hat{y})$ for T_{ct} (i), $\boldsymbol{D} \sim [-(a\cos k_x - b\cos k_y)\sin k_y \hat{x} + (b\cos k_x - a\cos k_y)\sin k_x \hat{y}]$ for T_{ct} (ii), and $\boldsymbol{D} \sim (\cos k_y \sin k_x + i\cos k_x \sin k_y)\hat{z}$ for T_{ct} (iii).

$\boldsymbol{k}$-dependence of the gap functions self-consistently from (9). Figure 3 shows the α-dependence of T_c for the singlet (T_{cs}) and the triplet (T_{ct}) superconductivity at $U = 5.5$. The solid line with closed squares is T_{cs} and the gap function for the spin-singlet pairing is roughly given by that with $d_{x^2-y^2}$ symmetry, $D_0 \sim (\cos k_x - \cos k_y)$. For the singlet pairing, this is the only one stable gap function, as in the case without the Rashba SO interaction [33]. The other lines in figure 3 are for the spin-triplet states, and calculated with the assumption that the $\boldsymbol{d}$-vector belongs to (i) the A_1 representation of the point group C_{4v}, (ii) B_1 and (iii) E, respectively. For these representations, the $\boldsymbol{d}$-vector is roughly of the form of

(i) $\boldsymbol{D}^{A_1} \sim (-\cos k_x \sin k_y \hat{x} + \cos k_y \sin k_x \hat{y})$,

(ii) $\boldsymbol{D}^{B_1} \sim [-(a\cos k_x - b\cos k_y)\sin k_y \hat{x} + (b\cos k_x - a\cos k_y)\sin k_x \hat{y}]$ with $a > b$,

(iii) $\boldsymbol{D}^{E} \sim (\cos k_y \sin k_x + i\cos k_x \sin k_y)\hat{z}$.

All of these gap functions are p-wave gap functions. Note that they are all different from the form $(\cos k_x - \cos k_y)\hat{\boldsymbol{\mathcal{L}}}_0$ for which the gap function Δ can be diagonalized with respect to the SO split bands and no inter-band pairing is realized [31, 35, 36, 37]. Thus, in the spin-triplet pairing states obtained in this calculation, there are always inter-band Cooper pairs. This is due to incompatibility between the symmetry of the pairing interactions and the symmetry of the Rashba SO interaction, as mentioned before. It should be also notified that the triplet states with $\boldsymbol{D}^{A_1}$ and $\boldsymbol{D}^{B_1}$ are time-reversal invariant, while the triplet state with $\boldsymbol{D}^{E}$ is not, but a chiral $p + ip$ state. This is easily seen as follows. For the state with $\boldsymbol{D}^{A_1}$ or $\boldsymbol{D}^{B_1}$, under time-reversal operation, the gap function for $\uparrow\uparrow$ pairs $\Delta_{\uparrow\uparrow}(\boldsymbol{k}) = -D_1(\boldsymbol{k}) + iD_2(\boldsymbol{k})$ is transformed as $-D_1(-\boldsymbol{k}) - iD_2(-\boldsymbol{k}) = \Delta_{\downarrow\downarrow}(\boldsymbol{k})$, and also, $\Delta_{\downarrow\downarrow}(\boldsymbol{k}) \to \Delta_{\uparrow\uparrow}(\boldsymbol{k})$. Thus, the $\boldsymbol{D}^{A_1}$ state and the $\boldsymbol{D}^{B_1}$ state are time-reversal invariant.

As can be seen in figure 3, T_{cs} is not so strongly affected by the Rashba SO

interaction. In contrast, $T_{c\mathrm{t}}$ is rapidly decreased, as α increases, especially for $\boldsymbol{D}^{\mathrm{E}}$. The direction of this $\boldsymbol{d}$-vector is not compatible with the Rashba SO interaction at all. For this case, the factor $G(k)G(-k)$ in eq.(9) can be negative on a wide area of the Fermi surface. Therefore, the direction of the $\boldsymbol{d}$-vector strongly tends to align in the xy-plane. On the other hand, the superconductivity described by the gap function $\boldsymbol{D}^{\mathrm{A}_1}$ is most stable for large α, because $\boldsymbol{\mathcal{L}}_0$ in the Rashba SO interaction, which tends to direct the $\boldsymbol{d}$-vector so that the condition $\boldsymbol{D} \parallel \boldsymbol{\mathcal{L}}_0$ is satisfied, belongs also to A_1 irreducible representation. In this sense, $\boldsymbol{D}^{\mathrm{A}_1}$ is, to some extent, compatible with the Rashba SO interaction, though it does not yet fully optimize the Rashba interaction, leading to strong inter-band pair correlations. In the case of $\boldsymbol{D}^{\mathrm{B}_1} \sim [(a\cos k_x - b\cos k_y)\sin k_y\hat{x} - (b\cos k_x - a\cos k_y)\sin k_x\hat{y}]$, the parameters a and b in the gap function changes as α is increased. For $\alpha = 0$, $(a, b) \propto (1, 0)$. When α is turned on, a is decreased while b increased so that $\boldsymbol{D}^{\mathrm{B}_1}$ would become close to the form compatible with $\boldsymbol{\mathcal{L}}_0$. This change is continuous with respect to α and the gap function $\boldsymbol{D}^{\mathrm{B}_1}$ is transformed gradually. As will be shown later in figure 5 and figure 6, $\boldsymbol{D}^{\mathrm{B}_1}$ has p-wave like character for small α and is gradually changed into the f-wave like gap function (i.e. $a = b$) as α is increased. As seen in figure 3, T_c for $\boldsymbol{D}^{\mathrm{B}_1}$ has a minimum around $\alpha \simeq 0.04$ and a hump around $\alpha \simeq 0.06$. This α-dependence is understood as follows. As mentioned before, T_c is determined by competition and interplay between the pairing interaction and the Rashba SO interaction. As α increases, because of the change of the electronic structure due to the Rashba SO interaction, the pairing interaction in the p-wave channel becomes weak in our model. This results in the overall decrease of T_c for $\boldsymbol{D}^{\mathrm{B}_1}$ state. On the other hand, the increase of α also changes the structure of the $\boldsymbol{D}^{\mathrm{B}_1}$ gap function more compatible with the Rashba SO interaction, suppressing inter-band pairings between the SO split bands and also associated pair-breaking effects. A slight increase for $0.04 < \alpha < 0.06$ is caused by this suppression of the inter-band pairings. In our model, for $\alpha > 0.1$, the decrease of T_c for $\boldsymbol{D}^{\mathrm{B}_1}$ is substantial. Thus, the pairing state with $a = b$, i.e. f-wave state, can not be realized.

3.3. Pairing state and transition temperature in the case with parity-mixing

The pairing states obtained in the previous subsection is drastically changed once we take into account the parity mixing of the singlet and the triplet gap functions. According to the behaviors of $T_{c\mathrm{s}}$ and $T_{c\mathrm{t}}$ in figure 3, the d-wave and the p-wave pairing states may be mixed through the Rashba SO interaction. For the admixture of the gap functions, however, only the gap functions which belong to the same irreducible representation of the point group are allowed to coexist. The p-wave gap function $\boldsymbol{D}^{\mathrm{A}_1}$ with the highest $T_{c\mathrm{t}}$ belongs to A_1 representation of C_{4v} and the d-wave gap function $D_0 \sim (\cos k_x - \cos k_y)$ to B_1. This implies that these two gap functions can not be mixed. Then, the next candidate is the admixture of the d-wave state and the p-wave state with $\boldsymbol{D}^{\mathrm{B}_1}$. The symmetry argument allows this admixture. Indeed, we found that the only one solution of eq.(9) is the $d+p(\mathrm{B}_1)$ wave state. Figure 4 shows the transition temperature T_c for this

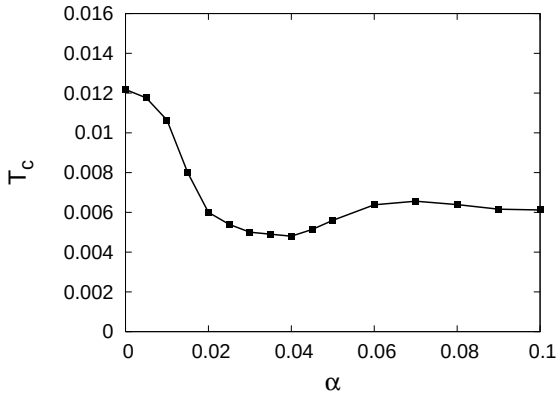

Figure 4. α versus T_c for the singlet and triplet mixed B_1 symmetric state at $U = 5.5$.

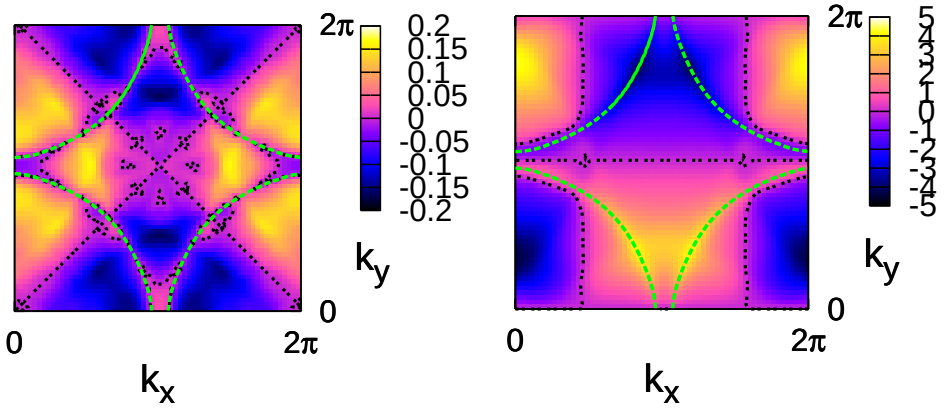

Figure 5. The gap functions for the $d+p(B_1)$ state plotted on (k_x, k_y) plane. $D_0(i\omega_n = i\pi T_c, \boldsymbol{k})$ (left panel) and $D_1(i\omega_n = i\pi T_c, \boldsymbol{k})$ (right panel) for $\alpha = 0.005, U = 5.5$. Green dotted lines indicate locations of the SO split Fermi surfaces. Black dotted lines indicate locations of gap nodes where the gap amplitude vanishes.

$d+p(B_1)$ wave superconductivity as a function of α. For small α, the superconductivity is dominated by the spin-triplet state, while for large α it is dominated by the spin-singlet state. For intermediate values of α, the two gap functions are strongly mixed with the same order of magnitude.

We show the $\boldsymbol{k}$ dependence of $D_0(i\pi T_c, \boldsymbol{k})$ and $D_1(i\pi T_c, \boldsymbol{k})$ for the $d + p(B_1)$ state in figure 5 for $\alpha = 0.005$ and in figure 6 for $\alpha = 0.1$. Note that $D_2(i\omega_n, k_x, k_y) = D_1(i\omega_n, k_y, k_x)$ is satisfied for the B_1 symmetric superconducting state. For small α, D_1 exhibits a conventional p-wave behavior, in the sense that the Fermi surfaces cross the nodal lines of D_1 only near $(\pm\pi, 0)$ and the amplitude of D_1 is much larger than that of D_0. Meanwhile, for large α, D_1 is more like a f-wave state in the sense that the Fermi surfaces cross the nodal lines of D_1 around $(\pm 0.4\pi, \pm 0.7\pi)$ in addition to $(\pm\pi, 0)$, though the single-particle energy is fully gapped with no nodal lines as will be clarified in the next section. The change from the conventional p-wave like gap function to the f-wave like one is continuous, and actually the f-wave like state should be classified

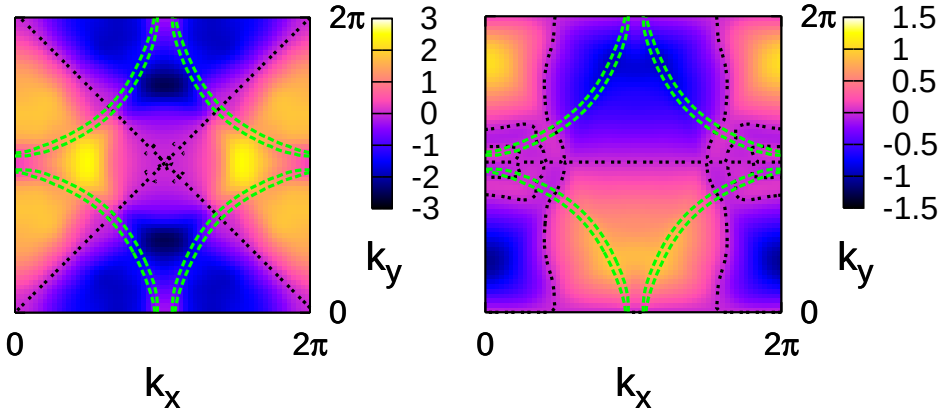

Figure 6. The gap functions for the $d+p(\mathrm{B}_1)$ state plotted on (k_x, k_y) plane. $D_0(i\omega_n = i\pi T_c, \boldsymbol{k})$ (left panel) and $D_1(i\omega_n = i\pi T_c, \boldsymbol{k})$ (right panel) for $\alpha = 0.1, U = 5.5$. Green dotted lines indicate locations of the SO split Fermi surfaces. Black dotted lines indicate locations of gap nodes where the gap amplitude vanishes.

as a p-wave state with higher harmonics. In our model, even for large $\alpha > 0.1$, $\boldsymbol{D}^{\mathrm{B}_1}$ does not change to the form $D_0\hat{\boldsymbol{\mathcal{L}}}_0$ (i.e. a genuine f-wave state) for which no inter-band pairing exists. This is because V_t does not favor such a structure of the d-vector. The two factors for the determination of the d-vector, the pairing interaction and the Rashba SO interaction, generally have different origins and favor different types of gap functions. Therefore, our results imply that, for the case that the pairing interaction in a spin-triplet channel is sufficiently strong, it is rather generally hard for the gap function to be compatible with the Rashba SO interaction, resulting in the existence of the inter-band pairing, in contrast to previous studies on simple models in which it is assumed that the spin-triplet pairing interaction compatible with the asymmetric SO interaction always exists [31, 35, 36]. In the case that the pairing interaction for the triplet superconductivity is very small compared with that for the singlet one and the asymmetric SO interaction, the triplet component is induced by the singlet component, hence $\boldsymbol{D} \parallel \hat{\boldsymbol{\mathcal{L}}}_0$ can be satisfied.

We note that the relative phase of $\boldsymbol{D}$ to D_0 is determined through the Rashba SO interaction. The eigenvalue of eq.(9) for $\Delta = (D_0 - \boldsymbol{D}\cdot\boldsymbol{\sigma})i\sigma_2$ where $(D_0, \boldsymbol{D})$ is the gap function illustrated in figures 5 and 6 is smaller than that for $\Delta = (D_0 + \boldsymbol{D}\cdot\boldsymbol{\sigma})i\sigma_2$. The resulting gap function has no degrees of freedom with respect to the relative phase between the singlet component D_0 and the triplet component $\boldsymbol{D}$.

As mentioned in the previous subsection, the $d+p(\mathrm{B}_1)$ pairing state is time-reversal invariant. Thus, the asymmetric SO interaction restores the time-reversal symmetry of the superconducting state, which is broken in the bulk of $\mathrm{Sr_2RuO_4}$ where the chiral $p+ip$ state is realized. This restored time-reversal symmetry bears an important implication for the realization of time-reversal invariant topological superconductivity, as will be discussed in the next section.

4. A possible realization of topological superconductivity

In this section, we present the scenario of the Z_2 topological superconductivity on the basis of the results obtained in the previous section. As mentioned in the introduction, the stability of the topological superconductivity is ensured by time-reversal symmetry and the existence of a full energy gap which separates the topologically nontrivial ground state from excited states [10, 12, 14, 15]; there should be no nodal lines of the gap, from which gapless excitations may emerge, destabilizing the gapless edge modes and destroying the topological phase. The time-reversal invariance is evident for our $d+p(\mathrm{B}_1)$ state, as mentioned in the previous section. Thus, we, here, examine whether the single-particle energy for the $d+p(\mathrm{B}_1)$ wave state is fully gapped, and there is no nodal lines of the gap. To simplify our analysis, we assume the BCS mean field Hamiltonian, which is, in the matrix form,

$$\begin{pmatrix} \varepsilon_k + \alpha \boldsymbol{\mathcal{L}}_0(\boldsymbol{k}) \cdot \boldsymbol{\sigma} & \hat{\Delta}_k \\ \hat{\Delta}_k^\dagger & -\varepsilon_k - \alpha \boldsymbol{\mathcal{L}}_0(-\boldsymbol{k}) \cdot \boldsymbol{\sigma}^t \end{pmatrix}, \tag{11}$$

with

$$\hat{\Delta}_k = D_0(\boldsymbol{k}) i\sigma_2 + \boldsymbol{D}(\boldsymbol{k}) \cdot \boldsymbol{\sigma} i\sigma_2, \tag{12}$$

where $D_0(\boldsymbol{k})$ is the spin-singlet gap, and $\boldsymbol{D}(\boldsymbol{k})$ is the $\boldsymbol{d}$-vector for the spin-triplet component. The energy eigen value of (11) is obtained as [41]

$$\begin{aligned} E_{k\pm} = [&\varepsilon_k^2 + \alpha^2 |\boldsymbol{\mathcal{L}}_0(\boldsymbol{k})|^2 + |\boldsymbol{D}(\boldsymbol{k})|^2 + D_0(\boldsymbol{k})^2 \\ &\pm 2\sqrt{(\varepsilon_k \alpha \boldsymbol{\mathcal{L}}_0(\boldsymbol{k}) + D_0(\boldsymbol{k})\boldsymbol{D}(\boldsymbol{k}))^2 + (\alpha \boldsymbol{\mathcal{L}}_0(\boldsymbol{k}) \times \boldsymbol{D}(\boldsymbol{k}))^2}]^{\frac{1}{2}}, \end{aligned} \tag{13}$$

and the minus branch of the eigen values $-E_{k\pm}$. When $\boldsymbol{D}(\boldsymbol{k}) \parallel \boldsymbol{\mathcal{L}}_0(\boldsymbol{k})$, the energy spectrum (13) is reduced to $E_{k\pm} = \sqrt{\varepsilon_{k\pm}^2 + \Delta_\pm^2(\boldsymbol{k})}$, with $\varepsilon_{k\pm} = \varepsilon_k \pm \alpha |\boldsymbol{\mathcal{L}}_0(\boldsymbol{k})|$ and $\Delta_\pm(\boldsymbol{k}) = D_0(\boldsymbol{k}) \pm |\boldsymbol{D}(\boldsymbol{k})|$. The energy spectrum is diagonal with respect to the SO-split-band-index $\pm$, and there are no inter-band Cooper pairs. For the $p+d$ wave state obtained in the previous section, $\boldsymbol{D}(\boldsymbol{k}) \parallel \boldsymbol{\mathcal{L}}_0(\boldsymbol{k})$ does not hold for a wide range of parameters. In this situation, the energy spectrum (13) is not diagonal with respect to the band index, which implies that there exist inter-band Cooper pairs as well as intra-band pairs. The condition for the existence of gapless excitations, $E_{k\pm} = 0$, is recast in,

$$\varepsilon_k^2 - \alpha^2 |\boldsymbol{\mathcal{L}}_0(\boldsymbol{k})|^2 + |\boldsymbol{D}(\boldsymbol{k})|^2 - D_0(\boldsymbol{k})^2 = 0, \tag{14}$$

$$\varepsilon_k D_0(\boldsymbol{k}) - \alpha \boldsymbol{\mathcal{L}}_0(\boldsymbol{k}) \cdot \boldsymbol{D}(\boldsymbol{k}) = 0. \tag{15}$$

$\boldsymbol{k}$-points at which the excitation energy gap closes should satisfy both eqs.(14) and (15). We examine these conditions numerically for the $d+p(\mathrm{B}_1)$ state. The calculations presented in the previous sections are valid only for $T \geq T_c$. Thus, for the evaluation of (14) which requires the magnitude of the gap function, we assume that the maximum values of the superconducting gaps D_0 and $|\boldsymbol{D}(\boldsymbol{k})|$ at $T = 0$ are obtained from the BCS mean field relation $\Delta/T_c = 1.764$. Using this approximation, we derive $\boldsymbol{k}$-points satisfying eqs.(14) and (15) for the $d+p(\mathrm{B}_1)$ state. The results for some values of α are

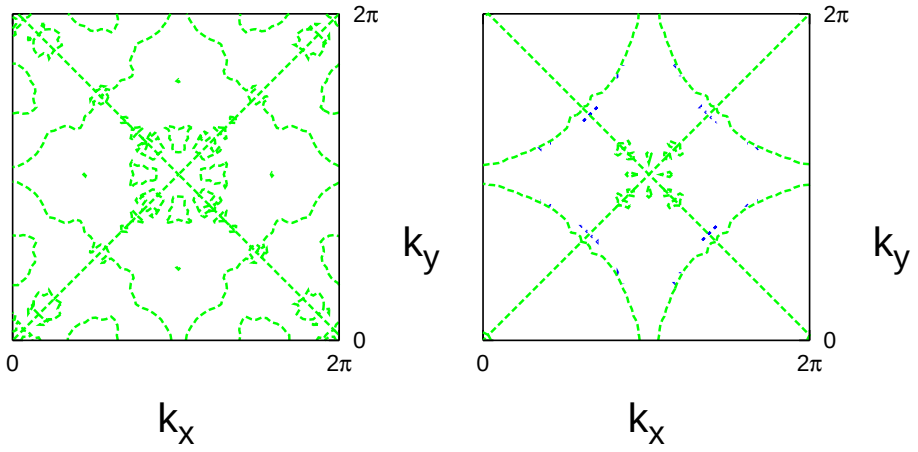

Figure 7. $\boldsymbol{k}$-points satisfying eqs.(14) (blue line) and (15) (green line) plotted for $\alpha = 0.005$ (left panel) and $\alpha = 0.02$ (right panel). For $\alpha = 0.005$, the left-hand side of (14) is larger than 0 in the entire Brillouin zone.

shown in figure 7. We found that when α is sufficiently small, the left-hand side of (14) is positive for all $\boldsymbol{k}$ in the entire Brillouin zone, and thus there are no gapless excitations. As α is increased from 0, the left-hand side of (14) decreases, and when α reaches to a value $\alpha_0 \sim 0.02$, eq.(14) is fulfilled in a certain region of $\boldsymbol{k}$ where $k_x \approx \pm k_y \approx \pm 0.65\pi$. The condition (15) is also satisfied exactly on the line $k_x = \pm k_y$, because of the B_1 symmetry; i.e. $D_1(-k_y, k_x) = D_2(k_x, k_y)$ and $D_0(k_x, k_x) = 0$. This implies that the gap collapses at certain $\boldsymbol{k}$-points on the line $k_x = k_y$. Our numerical data for the gap function indicate that this gap-closing does not occur for $0 < \alpha < \alpha_0$. For this parameter region, the bulk excitations have the full energy gap in the whole Brillouin zone, which is a necessary condition for the realization of the topological superconductivity.

We, next, consider the adiabatic deformation of the above $d + p(B_1)$ wave state to a topologically equivalent state. This deformation is achieved by changing parameters of the Hamiltonian without closing the bulk gap [10, 11]. Since any gradual changes of parameters cannot change the nonzero topological number which is discrete, the existence of the bulk gap ensures the topological stability of the state. As mentioned above, for $0 < \alpha < \alpha_0$, $\varepsilon_k^2 + |\boldsymbol{D}(\boldsymbol{k})|^2 > \alpha^2 |\boldsymbol{\mathcal{L}}_0(\boldsymbol{k})|^2 + D_0(\boldsymbol{k})^2 > 0$ holds. Thus we can change adiabatically the magnitude of the spin-singlet gap $D_0(\boldsymbol{k})$ and the strength of the SO interaction α to zero without closing the excitation gap. After this deformation, the system is equivalent to a combined system of a $p + ip$ state and a $p - ip$ state, which indeed exhibits the Z_2 topological superconductivity [14, 16, 17, 18]. As a result, the $d + p(B_1)$ wave state obtained in the section 3 is topologically equivalent to the Z_2 topological superconductivity.

In this Z_2 topological phase, there are counter-propagating gapless edge states, which are Majorana fermions [14, 18]. The Majorana edge states may give rise to intriguing transport phenomena associated with spin currents [42]. Since there is a diamagnetic supercurrent on the boundary surface, for the detection of the spin current

carried by edge quasiparticles, thermomagnetic effects may be utilized [18]. Also, the gapless edge quasiparticles may be observed as a zero bias peak of tunneling currents [17, 18].

5. Discussion and summary

In this paper, we have investigated pairing states realized at the (001) interface of Sr_2RuO_4 by using microscopic calculations based on the Kohn-Luttinger-type pairing mechanism. It is found that at the (001) interface of Sr_2RuO_4, the strong admixture of p-wave pairings and d-wave pairings realizes, and thus this system is suitable for the exploration of strong parity-mixing of Cooper pairs caused by broken inversion symmetry. An important implication of our results is as follows. When there are strong spin-triplet pairing correlations in NCSC, the frustration between the pairing interaction and the asymmetric SO interaction occurs quite generally, because of incompatibility between the pairing interaction and the symmetry of the asymmetric SO interaction. This yields substantial spin-triplet inter-band pairs between electrons in two SO split bands, even when the size of the SO split is considerably larger than the superconducting gap. Because of this feature, the most stable parity-mixed pairing state realized at the (001) interface of Sr_2RuO_4 is the $d+p(B_1)$ wave state, in which time-reversal symmetry is restored, in contrast to the bulk Sr_2RuO_4, which is believed to be in the chiral $p+ip$ state with broken time-reversal symmetry. Another intriguing conclusion drawn from our results is that this $d+p(B_1)$ wave state can be a promising candidate of the recently-proposed Z_2 topological superconductivity. That is, the $d+p(B_1)$ wave state is topologically equivalent to the state that consists of a $p+ip$ state for $\uparrow\uparrow$ pairs and a $p-ip$ state for $\downarrow\downarrow$ pairs, which supports the existence of counter-propagating gapless edge states carrying spin currents. This feature may be observed experimentally in the transport properties for heat currents and spin currents, as discussed in some literature [17, 18, 42].

Some concluding remarks are in order. For the spin-triplet pairing state obtained in the above analysis, inter-band pair correlation between the SO split bands is substantially large. This result for inter-band pairings implies that pairing states with center-of-mass momentum such as the Fulde-Ferrel-Larkin-Ovchinikov (FFLO) state [43, 44] may be more stabilized for some parameter regions compared to uniform states considered in the current paper. The stability of the FFLO state depends on competition between pairing interaction for this state and the cost of the kinetic energy due to the finite center-of-mass momentum. The issue of a possible realization of the FFLO state at an interface of Sr_2RuO_4 is quite intriguing, and should be addressed in the near future.

In the argument for the realization of the topological superconductivity presented in this paper, we did not consider effects of the bulk SO interaction due to the d-electron orbitals, but simply assumed that the asymmetric SO interaction overwhelms the bulk SO interaction in the vicinity of the interface. Actually, there should exist a domain

boundary between the chiral $p+ip$ state in the bulk governed by the bulk SO interaction and the time-reversal-invariant $p + d$ state near the interface. It is highly nontrivial how the interaction between these two states affects the stability of the topological superconductivity. However, it is expected that as long as the thickness of the region, where the asymmetric SO interaction is dominant, is sufficiently large compared to the coherence length of Cooper pairs, the topological superconductivity should be stable in the vicinity of the interface. Another point required for the realization of the topological superconductivity is the fabrication of the interface where the electronic structure is not so different from the bulk one. In the (001) surface of Sr_2RuO_4, however, it is known that a structural phase transition occurs and the surface state is ferromagnetic[45]. To observe the time-reversal symmetric superconductivity, a very carefully fabricated sample without such a structural phase transition is needed.

Acknowledgments

The authors have benefited from conversation with M. Sato and S. C. Zhang. Numerical calculations were partially performed at the Yukawa Institute for Theoretical Physics, Kyoto University. This work was partly supported by the Grant-in-Aids for Scientific Research from MEXT of Japan (Grant No.18540347, Grant No.19014009, Grant No.19014013, Grant No.19052003, Grant No.20029013, and Grant No.20102008) and the Grant-in-Aid for the Global COE Program "The Next Generation of Physics, Spun from Universality and Emergence". Y. Tada is supported by JSPS Research Fellowships for Young Scientists.

References

[1] Vollhardt D and Wölfle P 1990 *The Superfluid Phases of Helium 3* (Tayler & Francis)
[2] A. P. Mackenzie and Y. Maeno, Rev. Mod. Phys. **75**, 657 (2003).
[3] Rice T M and Sigrist M 1995 J. Phys. Cond. Matter **7** L643
[4] Volovik G E and Gorkov L P 1985 Sov. Phys. JETP **61** 843
[5] Sigrist M and Ueda K 1991 Rev. Mod. Phys. **63** 239
[6] Ishida K, Mukuda H, Kitaoka Y, Asayama K, Mao Z Q, Mori Y and Maeno Y 1998 Nature **396** 658
[7] Luke G M, Fudamoto Y, Kojima K M, Larkin M I, Merrin J, Nachumi B, Uemura Y J, Maeno Y, Mao Z Q, Mori Y, Nakamura H and Sigrist M 1998 Nature **394** 558
[8] Stone M and Roy R 2004 Phys. Rev. B **69** 184511
[9] Lee D H, Zhang G M, and Xing T 2007 Phys. Rev. Lett. **99**, 196805.
[10] Kane C L and Mele E J 2005 Phys. Rev. Lett **95** 146802
[11] Kane C L and Mele E J 2005 Phys. Rev. Lett **95** 226801
[12] Bernevig B A, Hughes T L, and Zhang S C 2006 Science **314** 1757
[13] König M, Wiedmann S, Brüne C, Roth A, Buhmann H, Molenkamp L, Qi X L, and Zhang S C 2007 Science **318** 766
[14] Roy R arXiv:0803.2868
[15] Roy R cond-mat/0608064
[16] Qi X L, Hughes T L, Raghu S, and Zhang S C arXiv:0803.3614
[17] Tanaka Y, Yokoyama T, Balatsky, and Nagaosa N Phys. Rev. B **79**, 060505(R) (2009)

[18] Sato M and Fujimoto S Phys. Rev. B **79**, 094504 (2009)
[19] Schnyder A P, Ryu Shinsei, Furusaki A, Ludwig A W W 2008 Phys. Rev. B **78** 195125
[20] Bauer E, Hilscher G, Michor H, Paul Ch, Scheidt E W, Gribanov A, Seropegin Yu, Noël H, Sigrist M, and Rogl P 2004 Phys. Rev. Lett. **92** 027003
[21] Akazawa T, Hidaka H, Kotegawa H, Kobayashi T, Fujiwara T, Yamamoto E, Haga Y, Settai R, and Ōnuki Y 2004 J. Phys. Soc. Jpn. **73** 3129
[22] Kimura N, Ito K, Saitoh K, Umeda Y, Aoki H, and Terashima T 2005 Phys. Rev. Lett. **95** 247004
[23] Sugitani I, Okuda Y, Shishido H, Yamada T, Thamizhavel A, Yamamoto E, Matsuda T D, Haga Y, Takeuchi T, Settai R, and Ōnuki Y 2006 J. Phys. Soc. Jpn. **75** 043703
[24] Togano K, Badica P, Nakamori Y, Orimo S, Takeya H, and Hirata K 2004 Phys. Rev. Lett. **93** 247004
[25] Badica P, Kondo T, and Togano K 2005 J. Phys. Soc. Jpn **74** 1014
[26] Hayashi N, Wakabayashi K, Frigeri P A, and Sigrist M 2006 Phys. Rev. B**73** 092508
[27] Yuan H Q, Agterberg D F, Hayashi N, Badica P, Vandervelde D, Togano K, Sigrist M, and Salamon M B 2006 Phys. Rev. Lett. **97** 017006
[28] Nishiyama M, Inada Y, Zheng G 2007 Phys. Rev. Lett. **98** 047002
[29] Izawa K, Kasahara Y, Matsuda Y, Behnia K, Yasuda T, Settai R, and Ōnuki Y 2005 Phys. Rev. Lett. **94** 197002
[30] Rashba E I Sov. Phys. 1960 Solid State **2** 1109
[31] Edelstein V M 1989 Sov. Phys. JETP **68** 1244
[32] Gorkov L P and Rashba E 2001 Phys. Rev. Lett. **87** 037004
[33] Nomura T and Yamada K 2000 J. Phys. Soc. Jpn. **69** 3678
[34] Nomura T and Yamada K 2003 J. Phys. Soc. Jpn. **72** 2053
[35] Frigeri P A, Agterberg D F, Koga A, and Sigrist M 2004 Phys. Rev. Lett. **92** 097001
[36] Fujimoto S 2007 J. Phys. Soc. Jpn. **76** 051008
[37] Fujimoto S 2007 J. Phys. Soc. Jpn. **76** 034712
[38] Ng. K. K. and Sigrist M 2000 Europhys. Lett. **49** 473
[39] Yanase Y and Ogata M 2003 J. Phys. Soc. Jpn. **72** 673
[40] Kohn W and Luttinger J M 1965 Phys. Rev. Lett. **15** 524
[41] Sato M 2006 Phys. Rev. B **73** 214502
[42] Vorontsov A B, Vekhter I, Eschrig M 2008 Phys. Rev. Lett. **101** 127003
[43] Fulde P and Ferrel R A 1964 Phys. Rev. **135** A550
[44] Larkin A I and Ovchinnikov Yu N 1964 Sov. Phys. JETP **20** 762
[45] Matzdorf R, Fang Z, Ismail, Zhang Jiandi, Kimura T, Tokura Y, Terakura K, and Plummer E W 2000 Science **289** 746